RSC Applied Interfaces

ROYAL SOCIETY OF CHEMISTRY

PAPER

View Article Online
View Journal | View Issue

Cite this: *RSC Appl. Interfaces*, 2024, **1**, 748

Surface modification of bioactive glasses for successful incorporation with poly(lactic-*co*-glycolic acid) (PLGA)†

Nishant Jain, [a] Johannes Schmidt,[b] Oliver Görke,[a] David Karl, [a] Aleksander Gurlo [a] and Franziska Schmidt ‡*[a]

Received 29th December 2023,
Accepted 22nd March 2024

DOI: 10.1039/d3lf00273j

rsc.li/RSCApplInter

Bioactive glass (BG)–polymer composites are promising materials for bone grafting in bone tissue regeneration. BG provides rigidity and can initiate bone growth, whereas the polymer matrix provides flexibility and biocompatibility. However, due to the complex composition of BG, incorporation into the polymer matrix is difficult and often leads to unwanted porosity and low interface strength between both components. In this study, we investigate the surface treatment of commercially available micronized melt-derived BG with varying compositions (45S5 and 1393) to improve its incorporation into a poly(lactic-*co*-glycolic acid) (PLGA) matrix by improving surface roughness, surface charge and active sites on the BG. The surfaces of BG are modified by treatment in simulated body fluid (SBF) for 3 days prior to composite production. This leads to the formation of carbonated hydroxyapatite on the surface of both BG types, as demonstrated by XRD, FTIR, XPS and EDX. This also leads to a change in surface texture and an increase in specific surface area from initially 3 to 116 $m^2\ g^{-1}$ and from 2 to 65 $m^2\ g^{-1}$ for 45S5 and 1393, respectively. Subsequently, composite PLGA–BG microspheres are fabricated using a probe-ultrasonication assisted solid-in-oil-in-water emulsion method. Additionally, the surface interaction of bioactive glasses with PLGA is discussed in detail.

Introduction

Bioactive glasses (BGs) are a special subclass of bio-ceramic materials, as they are in an amorphous state with increased solubility compared to crystalline materials. They are mostly silicate-based, and in rarer cases, phosphate or borate-based. Due to their high bioactivity, when introduced into the human body, they release ions and develop a crystalline carbonated hydroxyapatite (CHA) layer on the surface, encouraging cell adhesion and facilitating bone bonding. CHA is a naturally occurring mineral in bones that interacts with bone cells or can be degraded by osteoclasts.[1,2] Moreover, specific therapeutic ions like copper can be incorporated into melt-quenched bioactive glass which can induce angiogenesis.[3] The most widely used bioactive glass is Bioglass 45S5, developed by Larry L. Hench in 1969.[4] It was the first human-made material to bond with bone tissues. 45S5 is a silica-based glass composed of 45 wt% SiO_2, 24.5 wt% Na_2O, 24.5 wt% CaO, and 6 wt% P_2O_5. However, 45S5 bioglass has two main drawbacks: i) the processing can be challenging due to its low sinterability and high affinity for recrystallization and ii) in an aqueous surrounding, sodium ions (Na^+) are released in a burst, which leads to a local increase in pH in the surrounding tissue and may have cytotoxic effects.[5] Due to this, different glass compositions have been developed since, such as 1393,[6] ICIE16 (ref. 7) and others[8] with improved sinterability or reduced sodium content. The expected reactivity of a glass is related to its composition and network connectivity (NC). The NC of a glass is dependent mostly on the number of network formers (in the case of 45S5 and 1393 SiO_2 and P_2O_5, in the case of 1393, possibly also MgO) *vs.* network modifiers. 45S5 is a bioactive glass with a silicate NC of 2.11, while 1393 has a NC of 2.59.[9]

BGs are ideal for synthetic bone grafts as they easily bond with bone tissue cells and have shown bonding to soft tissues. To overcome their brittle nature, one approach to introduce elasticity into scaffolds is to disperse glass particles in a matrix of biologically compatible organic materials, such as polyesters, chitosan, and alginates.[10] Due to their overall processability,

[a] *Chair of Advanced Ceramic Materials, Institute of Material Science and Technology, Faculty III Process Sciences, Technische Universität Berlin, Straße des 17. Juni 135, 10623 Berlin, Germany. E-mail: franziska.schmidt2@charite.de*
[b] *Department of Chemistry, Division of Functional Materials, Technische Universität Berlin, Hardenbergstr. 40, 10623 Berlin, Germany*

† Electronic supplementary information (ESI) available. See DOI: https://doi.org/10.1039/d3lf00273j

‡ Currently at: Department of Prosthodontics, Geriatric Dentistry and Craniomandibular Disorders, Charité-Universitätsmedizin Berlin, Corporate Member of Freie Universität Berlin, Humboldt-Universität zu Berlin, and Berlin Institute of Health, 14197 Berlin, Germany

the resulting composites are of great interest for producing tissue engineering scaffolds, as they are thermoplastic and can be processed *via* a range of techniques, such as additive manufacturing.[11] More recently, composite powders have been employed in laser-based powder bed additive manufacturing (PBF-LB), with *e.g.*, poly(L-lactic acid) (PLA)/CHA[12] or PLA/hydroxyapatite microspheres.[13] Another commonly used matrix polyester is poly(lactic-*co*-glycolic acid) (PLGA), which is biodegradable, has FDA approval and generally has a lower melting point than pure PLA. The resulting composites would be bioresorbable and bioactive.[14] Specifically, powders made of spherical PLGA composite microsphere particles with bioactive glasses as fillers have great potential for many processes and applications, such as PBF-LP.[15]

However, bioceramic/BG–polymer composites show low interfacial bonding strength between the hydrophobic polymer matrix and hydrophilic bioceramic particles,[16] which can be addressed by using surface functionalization.[11] A common functionalization is surface silanization of bioceramics.[17]

In our previous work, we investigated the incorporation of 45S5 bioactive glass into PLGA to produce composite powders for PBF-LB of scaffold materials.[15] We observed that employing 45S5 without prior silanization led to porous PLGA microspheres without any incorporated BG. Silanization with *n*-PTES led to successful adhesion of 45S5 particles to the PLGA microsphere surface, which allowed us to produce composite powders with various 45S5 contents.

A less common functionalization with simulated body fluid (SBF) was successfully employed by Qiu *et al.*[18] to produce composite PLA/45S5 microspheres. Here the treatment of 45S5 in SBF led to the formation of CHA on the surface which then facilitated successful incorporation into the PLA matrix.

While 45S5 is the most bioactive glass with strong release kinetics for different alkali and alkaline earth metal ions (Na^+ and Ca^{2+}) and therefore with fast CHA formation on the surface, other silica based bioactive glasses with variations in alkali and alkaline earth metal content (such as 1393, ICIE16, F0, FastOS) show slower release kinetics especially for Na^+ and therefore slower change in pH. Hence, different bioactive glass chemistries might have different effects on incorporation. Conoscenti *et al.*[19] investigated the properties of composite PLA–BG scaffolds by a thermally induced phase separation method with 45S5 and 1393 as inorganic fillers and found that the presence of 45S5 altered the nucleation rate and growth process of the porous PLA matrix. This effect was not found in the presence of 1393. They related this to the fast release of ions from 45S5 during the synthesis. In addition, they found a significantly higher compressive Young's modulus in the composite scaffolds with 1393-BG compared to pure PLA and 45S5-BG containing composites. This study shows that the glass composition and release kinetics have a strong influence on the properties of the composite material.

Yet to the best of our knowledge, the effect of SBF treatment on the BG surface and the subsequent composite powder production process has not been investigated.

Therefore, in this study, we induce changes in the surface composition and morphology of commercially available 45S5 and 1393 BGs by treatment in simulated body fluid. We hypothesize that surface modification of bioactive glass will improve the incorporation into a PLGA matrix to produce biodegradable composite microspheres.

Materials and methods

Materials

In this study, the following materials are used as purchased without further purification: Bioglass® 45S5 (Schott Vitryxx, Schott AG, Mainz, Germany, d_{50} = 1.95 μm), bioactive glass 1393 (Schott, d_{50} = 3.15 μm), poly(lactic-*co*-glycolic acid) (PLGA) (Resomer® RG755S, Evonik), dichloromethane (DCM, Merck), polyvinyl alcohol (PVA Mwt = 60k, Merck), sodium chloride (NaCl, 95%, Roth), sodium hydrogen carbonate ($NaHCO_3$, Merck), potassium chloride (KCl, Merck), potassium hydrogen phosphate ($K_2HPO_4{\cdot}3H_2O$, Roth), magnesium chloride ($MgCl_2{\cdot}6H_2O$, Carl Roth), hydrochloric acid (HCl, 37%, Alfa), calcium chloride ($CaCl_2$, Merck), sodium sulfate (Na_2SO_4, Merck), and Tris buffer ($C_4H_{11}NO_3$, AppliChem).

Methods

SBF modification of 45S5 and 1393. SBF solution was prepared according to Kokubo *et al.*,[20] with 45S5 and 1393 bioactive glasses each treated in SBF as follows: 0.75 g of glass powder was treated in 300 ml of SBF solution in a plastic container at 37 °C for three days under constant stirring at 500 rpm. The modified bioactive glasses were centrifuged three times with double-distilled deionized water, followed by lyophilization for 24 hours.

Production of PLGA–bioactive glass (45S5 and 1393) microspheres. Composite PLGA–BG microspheres were produced by a solid-in-oil-in-water (s/o/w) emulsion method, as described previously in Karl *et al.*[15] To produce the water phase, 3.0 g of PVA was dissolved in 1 L of double-distilled deionized water at 80 °C for 24 hours under constant stirring at 1000 rpm.

PLGA dissolved in dichloromethane (DCM) was employed as the oil phase. For the solid-in-oil phase, 0.5 g of PLGA and 20 wt% of 45S5 and 1393 bioactive glasses (as received and SBF modified) were added to 2.5 ml DCM in an airtight glass container. The PLGA was dissolved under constant stirring using a magnetic stirrer at 500 rpm at room temperature (~25 °C).

To produce an emulsion, the solid-in-oil mixture was pipetted slowly into 80 ml of 0.3% PVA solution under constant ultrasonication (20 kHz) for 5 minutes. The formed emulsion was further subjected to constant stirring at 500 rpm for 4 hours at 22 °C with a magnetic stir bar to remove the solvent DCM. The obtained composite microspheres were washed three times using double-deionized distilled water in a centrifuge. The washed composite microspheres were freeze-dried for 24 hours to remove moisture and the remaining solvent.

Bioactive glass and composite microsphere characterization

Scanning electron microscopy (SEM)/energy dispersive X-ray detection (EDX). The surface morphology of the as-obtained and SBF-treated bioactive glass and PLGA–bioactive glass composite microspheres was examined on a scanning electron microscope coupled with an energy dispersive X-ray detector (SEM/EDX, ZEISS LEO GEMINI 1530, Germany). For this, the powder samples were fixed on conductive carbon tape on a sample holder and sputter coated with gold for 60 s to improve surface conductivity. For EDX quantification of the elemental composition, each sample was investigated by "point and shoot", meaning that the EDX spectrum was determined at one specific point. This was conducted in six different areas for each powder. From this, the elemental composition's mean values and standard deviations in at% were calculated. For the composite microsphere powders, EDX mapping was performed to determine the distribution of bioactive glass in the polymer matrix.

Surface roughness measurement. The change in surface roughness on BG single particles was measured on a Phenom XL scanning electron microscope (ThermoFisher Scientific, Waltham, MA, USA). The samples were fixed on a metal stub using double-sided conductive adhesive tape. The samples were imaged in low vacuum mode at 0.1 Pa to prevent charging. They were randomly scanned and photographed at different magnifications, and 3-dimensional heat maps were obtained.

Attenuated Fourier transform spectroscopy (ATR/FTIR). The chemical composition of the bioactive glasses before and after surface treatment was measured using Fourier transform infrared spectroscopy (FTIR, Bruker EQUINOX 55, USA) under air conditions in attenuated total reflection (ATR) mode in the IR region from 4000–400 cm^{-1}.

Powder X-ray diffraction (PXRD). The phase composition of the as-obtained and SBF-treated bioactive glasses was determined using powder X-ray diffraction (PXRD) on a D8 diffractometer (Bruker, Germany) with Co-Kα radiation in Bragg–Brentano mode with a scanning rate of 0.02.

X-ray photoelectron spectroscopy (XPS). X-ray photoelectron spectroscopy (XPS) measurements were carried out using a ThermoScientific K-Alpha+ X-ray photoelectron spectrometer with Al Kα radiation, and C 1s (284.8 eV) was used to calibrate the binding energies of the elements. All the samples were analyzed using a micro-focused, monochromatic Al Kα X-ray source (1486.68 eV; 400 μm spot size). The analyzer had a pass energy of 200 eV (survey) and 50 eV (high-resolution spectra), respectively. The K-Alpha+ charge compensation system was employed at all measurements to prevent any localized charge build-up during analysis. The samples were mounted on conductive carbon tape, and the resulting spectra were analyzed using the Avantage software from ThermoScientific.

N_2 adsorption–desorption isotherms. The N_2 adsorption–desorption isotherms of the as-received and SBF-treated bioactive glasses were analyzed in a Quadrasorb station (Quantachrome Instruments, USA) and determined by the Brunauer, Emmett and Teller (BET) method. All the samples were outgassed for 10 hours at 80 °C before the measurement.

Zeta potential. Changes in the surface potential of the bioactive glasses were determined using a Zetasizer (Malvern Instruments DTS 5200). For the measurement, 1.0 g of the sample was dispersed in 20 ml of physiological saline solution (9 g of NaCl in 1000 ml of deionized distilled water) and sonicated for 5 minutes to ensure homogeneous dispersion. All measurements were performed at neutral pH (7.4).

Particle size analysis (PSA). The particle size analysis (PSA) of PLGA and PLGA–bioactive glass composite microspheres were measured using a particle size analyzer (LS 13320, Beckman Coulter, Germany). For a typical measurement, particles were dispersed in water and sonicated for one minute.

Results and discussion

Chemical and physical analysis of bioactive glasses

PXRD showed that both as-delivered bioactive glasses (45S5 and 1393) were X-ray amorphous, as shown in Fig. 1(a). SBF treatment for three days led to the formation of carbonated hydroxyapatite (CHA; PDF19-0272) in both glasses. The

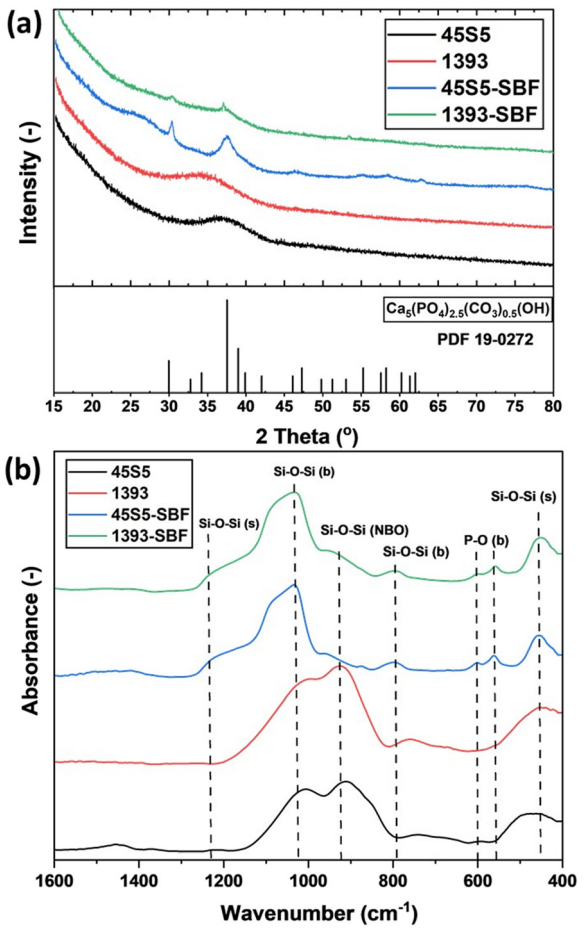

Fig. 1 (a) PXRD patterns and (b) ATR-FTIR spectra of the as-received and SBF-modified bioactive glasses.

higher intensity of reflections assigned to CHA in SBF-treated 45S5 compared to SBF-treated 1393 could be due to the larger amount of crystalline CHA in these samples, which in turn is an indicator of the higher bioactivity of SBF-treated 45S5. Fig. 1(b) shows the ATR-FTIR absorption bands for the as-delivered and SBF-treated bioactive glasses 45S5 and 1393. For the as-delivered BGs, absorption bands at 450 cm^{-1} and 910 cm^{-1} were found, which can be assigned to symmetric Si–O–Si vibration and non-bridging oxygen (NBO), formed through the glass network modifier creating Si–O groups. The broad absorption band at 1020 cm^{-1} (v_{assy}, Si–O–Si) can be assigned to the vibration of isolated $[SiO_4]$ tetrahedra.[3] After 3 days of immersion of the bioactive glasses in SBF solution, two absorption bands at 560 cm^{-1} and 600 cm^{-1} appear, which depict the bending mode of P–O–P bonds. This indicates apatite formation on the surface of the bioactive glasses. In addition, the shoulder at ~1230 cm^{-1} shows the formation of new Si–O–Si bonds from condensation of Si–OH groups. The appearance of this band correlates with the decrease of NBO at 910 cm^{-1}. The small band at 800 cm^{-1} appears due to 3D silica structure (δ Si–O–Si) development after 3 days of immersion.[10]

Elemental analysis by EDX, as shown in Fig. S1,† revealed the presence of Ca, P, Na, and Si in 45S5 and Mg and K as additional components in 1393, which is in agreement with the elemental composition of the glasses determined by Maçon *et al.*[21] In addition, the elemental composition of the glasses after SBF treatment was measured as well. XPS survey analysis also revealed the same as given in Fig. S2.†

The Ca/P atomic% ratio was determined by EDX analysis (each measurement is the average of six different areas per sample) and XPS, as shown in the values given in Table 1. It is clear that the Ca content decreases and the P content increases. Depending on the specific hydroxyapatite formation, the expected Ca/P ratio should change to 1.67 or 2.0.[22] In this study, XRD showed the formation of carbonated hydroxyapatite (Fig. 1a), which has a Ca/P relationship of 2.0. In addition, a decrease in Na content and an increase in P content in both the bioactive glasses and a decrease in K in 1393 are visible in the EDX spectra, proving a change in the surface elemental composition of the SBF-treated bioactive glasses (Fig. S1 and Table S1†). To take a deeper look into the calcium and phosphate amounts on the surface of the as-received and SBF-treated bioactive glasses, high-resolution XPS analysis was conducted as shown in Fig. 2. All calcium peaks (*i.e.*, Ca $2p_{3/2}/2p_{1/2}$ doublet) can be assigned to Ca^{2+}.[23] No significant peak shifts were observed after the surface treatment with SBF. The increasing amount of phosphorus (*i.e.* $[PO_4]^{3-}$) as mentioned in Table 1 on the surface is attributed to the adsorption of phosphates from SBF solution onto the bioactive glass surface.

Table 1 Peak fit table of Ca 2p and P 2p of the as-received and surface modified bioactive glasses

Bioactive glasses	Ca 2p	P 2p	Binding energy (eV)	Atomic%
45S5	Ca $2p_{3/2}$	—	346.8	86.72
	Ca $2p_{1/2}$	—	350.3	—
	—	P $2p_{3/2}$	132.5	13.28
	—	P $2p_{1/2}$	133.4	—
45S5-SBF	Ca $2p_{3/2}$	—	346.8	62.81
	Ca $2p_{1/2}$	—	350.3	—
	—	P $2p_{3/2}$	132.5	37.19
	—	P $2p_{1/2}$	133.4	—
1393	Ca $2p_{3/2}$	—	346.9	85.43
	Ca $2p_{1/2}$	—	350.5	—
	—	P $2p_{3/2}$	132.7	14.57
	—	P $2p_{1/2}$	133.6	—
1393-SBF	Ca $2p_{3/2}$	—	346.9	58.99
	Ca $2p_{1/2}$	—	350.5	—
	—	P $2p_{3/2}$	132.7	41.01
	—	P $2p_{1/2}$	133.6	—

The zeta potential of both bioactive glasses (45S5 and 1393) was determined to compare the change in the surface charge of the as-delivered and SBF-treated bioactive glasses (45S5 and 1393). The zeta potential of the as-delivered glasses at pH 7.4 is highly negative, as shown in Table 2 and shifts to −3.7 ± 2.7 mV after three days of SBF treatment for 1393 and 0.4 ± 1.1 mV for 45S5 (zeta potential distribution is given in Fig. S3†). The surface reaction on the bioactive glass rearranges the ions in the double layer and changes the reaction dynamics at the glass–solution interface.[24] The electrical charge moves towards positive values due to the accumulation of calcium ions on the surface of the bioactive glasses. The selective combination of the OH^- charged surface with the Ca^{2+} ions from the SBF solution occurs.[25]

This effect causes an overall positive charge on the surface of the bioactive glass. However, in our case, the zeta potential after SBF modification was more neutral and not extremely positive due to the adsorption of PO_4^{3-} from SBF solution onto the surface of the glass over time which neutralizes with Ca^{2+} on the surface.

Surface texture analysis of untreated and SBF-treated BGs

Fig. 3 shows the scanning electron micrographs (SEM) and the corresponding three-dimensional heat maps of single particles of the as-received bioactive glasses and SBF-treated bioactive glasses. The unmodified particles have a smooth surface with a plate-like morphology. The SBF-treated glass particles show a cauliflower-like morphology on the surface of the particles, which leads to an apparent increase in surface roughness due to the CHA formation on their surface. However, the quantification of surface roughness values is not comparable due to the wide particle size distribution, irregular shapes and also the presence of small particles and agglomerates on the surface of these glasses. N_2 gas adsorption–desorption isotherms were analyzed, which depicted mesoporous growth of CHA on the surface of the bioactive glasses; perhaps this can also be attributed to the increase in surface roughness of glass particles (see Fig. 3(e) and (f)).[26] SBF-treated 45S5 showed a higher volume of gas adsorption than SBF-treated 1393, which is supported by the change in the specific surface area (SSA) of the glasses after SBF treatment. The higher SSA of SBF-treated 45S5 (116 $m^2\ g^{-1}$) as compared to that of SBF-treated 1393 (65 $m^2\ g^{-1}$) is also

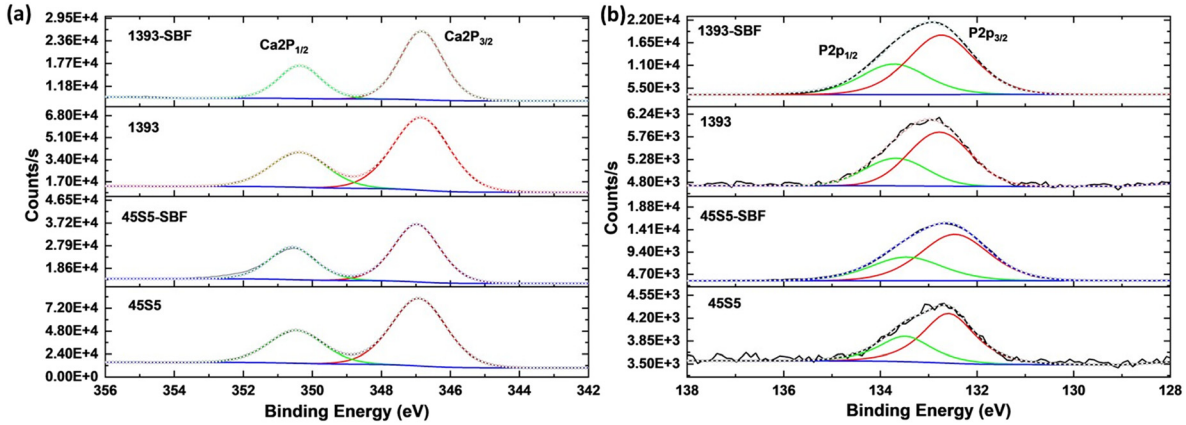

Fig. 2 (a) Ca 2p and (b) P 2p high resolution XPS spectra of the as-received and SBF-modified bioactive glasses.

attributed to the higher CHA growth and inadvertently better bioactivity of the 45S5 bioactive glass. As described previously, 45S5 has a silicate NC of 2.11, while 1393 has a NC of 2.59. A lower NC value relates to a more open silica network, which means higher solubility of the glass, which directly relates to bioactivity. Since 1393 has a higher NC, ion release is slower, as the silica network is stronger, and thus, the CHA growth is lower than that of 45S5 after 3 days of SBF treatment.[27]

Characterization of PLGA microspheres and PLGA–BG composite microspheres

PLGA microspheres and PLGA–bioactive glass composite microparticles were fabricated by an ultrasonication-assisted solid-in-oil-in-water emulsion method. Ultrasonication induces vibrations which help to divide bigger oil droplets into smaller ones. As a result, smaller microspheres can be generated. The viscosity of the polymer solution, the water phase to oil phase ratio and, most importantly, the energy input in the form of ultrasonication play key roles in the particle shape, size and yield. Therefore, particle size distribution and scanning electron microscopy are important to understand the shape and size of the produced microspheres.

Pure PLGA microspheres produced were spherical as shown in Fig. 4(a) having a particle size of 4.2 μm (d_{50}) (see Table 3). This small particle size is strongly related to parameters during the emulsion process, such as the energy input during emulsification, the polymer concentration in the oil phase and the oil-to-water-phase ratio.[28] In our case, we chose a high energy input by ultrasonication at 20 kHz, compared to stirring at 490 rpm in our previous study, where we produced pure PLGA microparticles with a d_{50} value of 40 μm.[15] The composite microspheres fabricated with the as-received bioactive glasses showed poor incorporation of filler particles (45S5 and 1393) in the polymer matrix as depicted in the SEM micrographs in Fig. 4(b) and (c). Unmodified 45S5 was not incorporated into the polymer matrix and led to the formation of porous PLGA microspheres (Fig. 4(b)). In the case of unmodified 1393, the SEM images showed larger BG particles separated from the polymer matrix forming agglomerated PLGA microspheres (Fig. 4(c)).

After SBF modification of both bioactive glasses, the filler incorporation improved, as depicted in the SEM micrographs in Fig. 4(d) and (e). In addition, some residual bioactive glass particles which did not adhere to the surface can also be seen as the composite powders were not sieved after drying. Incorporation of SBF modified BG into composite microspheres was investigated by SEM–EDX mapping, Fig. 5(a) and (b). EDX mapping showed uniform distribution of Ca and Si in the composite powder in the case of SBF-45S5 PLGA and SBF-1393 PLGA.

From the present study, it can be observed that when weak interaction between the filler and polymer matrix occurs, the polymer microspheres desorb from the interface and get separated, ruptured, or punctured during desorption from the glass. On the other hand, when there is a strong interaction between the filler and the polymer matrix, the spherical geometry of the composite microspheres is compromised to maintain the interfacial area.[29] The uniform and narrow particle size distribution of the composite (as shown in Fig. S4†) microspheres of the SBF-modified bioactive glasses with PLGA also supports good adsorption of the filler with the polymer matrix. For SBF-45S5 PLGA microspheres, 50% of the particles are less than 46.4 μm and for SBF-1393 PLGA, the d_{50} value is 9.9 μm. This size will likely be influenced by changes in the emulsion synthesis parameters, such as lower energy input or changes to the polymer concentration.

Table 2 Composition of the as-received and surface-treated bioactive glasses

Bioactive glasses	Ca/P atomic% ratio		Zeta potential ± error (mV)
	EDX	XPS	
45S5	5.9	6.53	−34.3 ± 1.7
45S5-SBF	2.19	1.68	0.4 ± 1.1
1393	6.5	5.86	−28.8 ± 4
1393-SBF	1.9	1.43	−3.7 ± 2.7

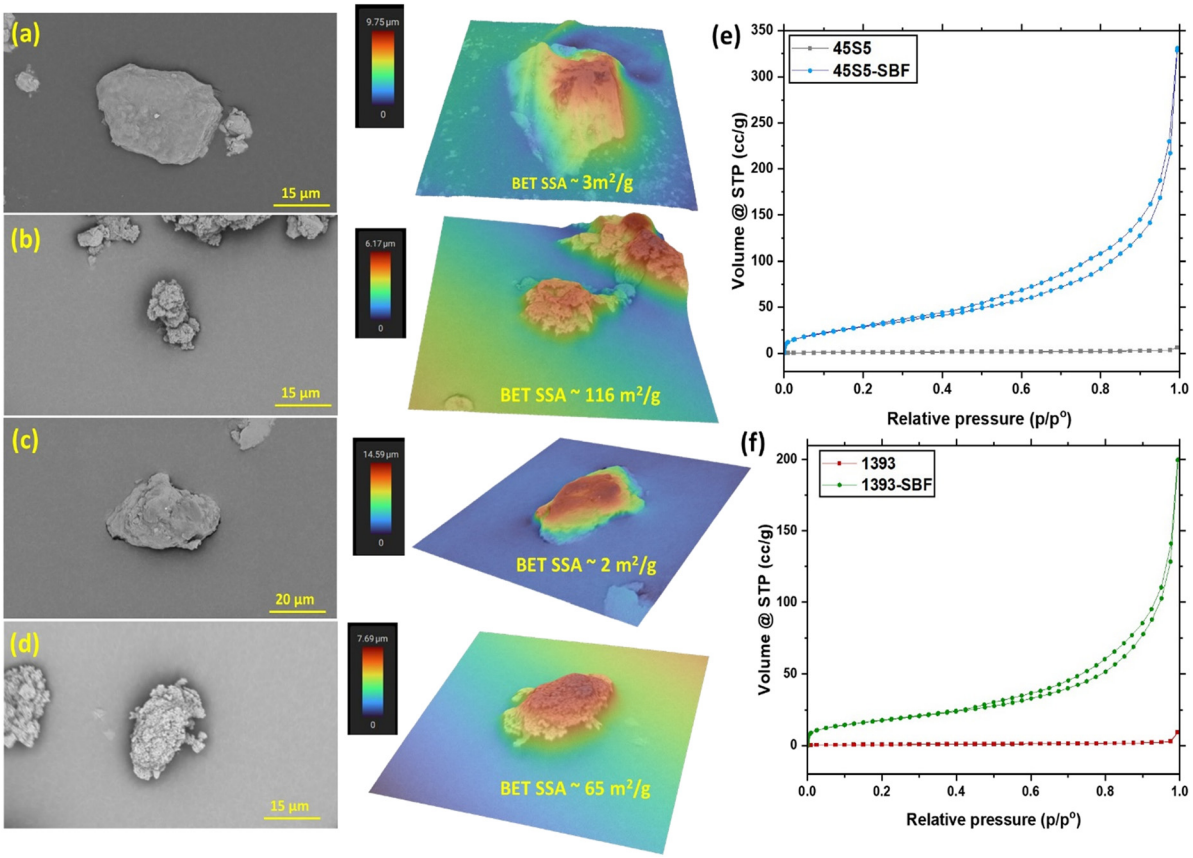

Fig. 3 SEM images and corresponding heat maps showing the surface roughness on glass particles as a result of the carbonated hydroxyapatite growth after immersion in SBF solution. This also contributes to the increase in BET-SSA (m^2 g^{-1}) of the following glasses (a) 45S5 (SEM magnification: 9500×, heat map field of view: 37.92 μm), (b) 45S5-SBF (SEM magnification: 10 000×, heat map field of view: 29.19 μm), (c) 1393 (SEM magnification: 7100×, heat map field of view: 41.166 μm) and (d) 1393-SBF (SEM magnification: 11 000×, heat map field of view: 30.37 μm). (e) and (f) N_2 adsorption–desorption isotherms of the as-received and SBF-modified bioactive glasses.

Surface interaction between bioactive glass and PLGA

A single composite microsphere with SBF-modified bioactive glass as shown in Fig. 6 depicts that bioactive glass particles have been adsorbed on the surface of the PLGA matrix. In our previous research, we compared PLGA–BG composite microspheres fabricated with the as-received BG, *n*-propyltriethoxysilane (PTES) treated BG, milled BG and *n*-PTES + milled BG. The results showed that composites with milled *n*-PTES coated BG did not show any obvious porosity, and milling and surface-treatment of the BG particles led to adhesion to the surface of the polymer microparticles.[15] Thereby, it was the best-suited feedstock for laser powder bed fusion additive manufacturing (LB-PBF).[6] As a result, this shows that it is essential to modify the surface of bioactive glass irrespective of its composition to improve its incorporation in the polymer matrix during composite microsphere production in the solid-in-oil-in-water emulsion process. The polymer interaction with flat surfaces was subjected to intensive experimental and theoretical studies.[30] However, very little research is available on polymer interaction with complex interfaces. Regarding bioactive glass substrates, Blaker *et al.*[31] investigated the surface wetting of bioactive glasses with biodegradable copolymers like PLGA and PDLLA but in a melt state. The biological interaction and bone growth behavior of bioactive glasses and their polymer composites have been established and proven again with extensive studies.[32,33] Nevertheless, the fundamental chemical and physical interaction between copolymers like PLGA and complex composition materials like bioactive glasses during the emulsion process has not been discussed before. Neuendorf *et al.*[34] explored the adhesion between various FDA approved biodegradable polymers like poly(L-lactide), poly(D-lactide), poly(DL-lactide), 75/25 PDL/polyglycolide, 50/50 PDL/polyglycolide and poly(ε-caprolactone) with hydroxyapatite. They concluded that the interactions between polymers and ceramics are controlled by purely physical interactions. In addition, Yan *et al.*[35] fabricated PLA–nano hydroxyapatite composite microspheres. With support from FTIR analysis, they claimed that the interaction between PLA and nano-hydroxyapatite was purely physical and not chemical, as no ionic interaction between Ca^{2+} and the carboxyl group (–COOH) occurred. In contrast, Hu *et al.*[36] claimed, based on FTIR results, that there was ionic bonding between the positive calcium ions and negative

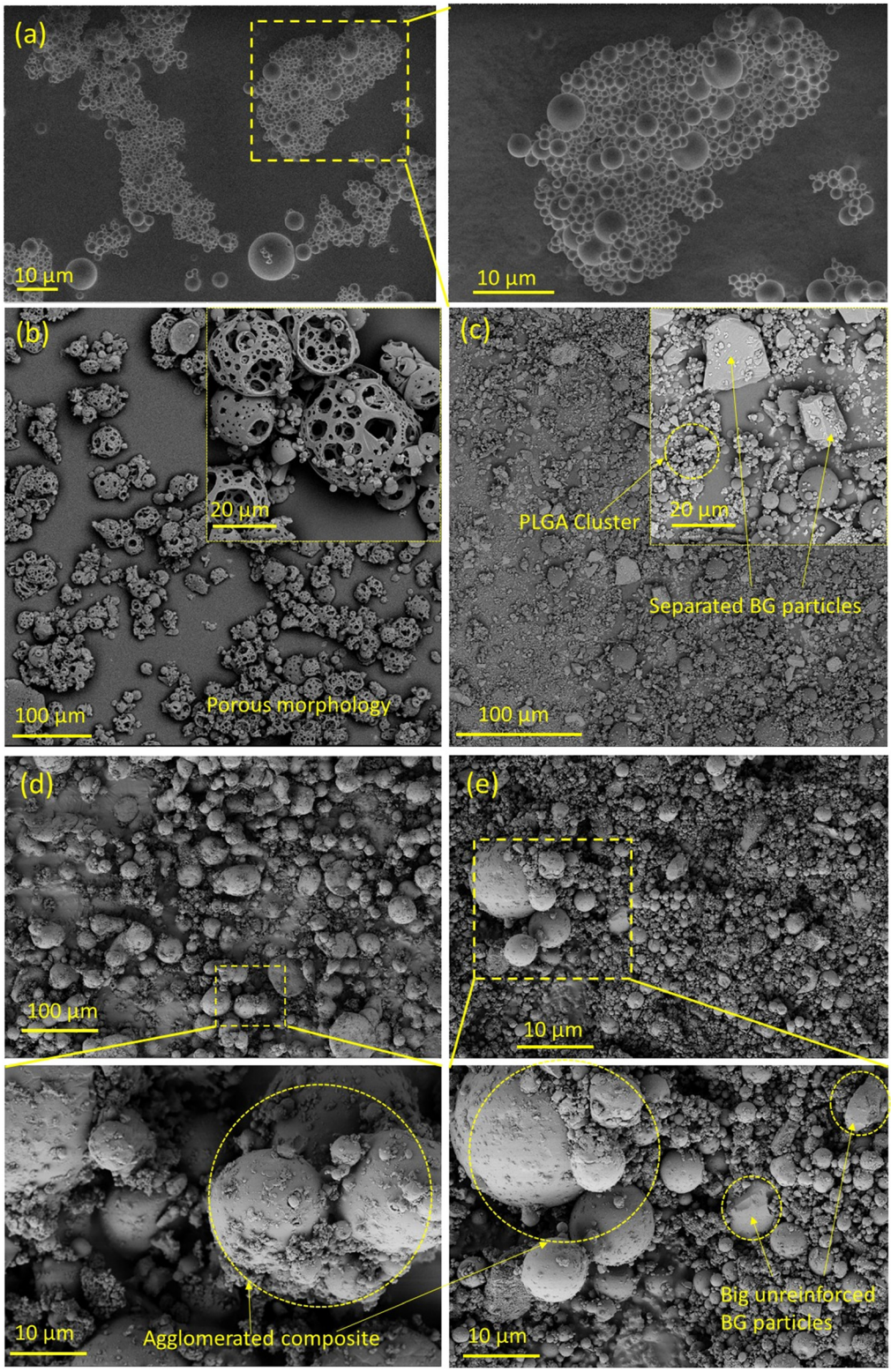

Fig. 4 SEM micrographs of (a) PLGA (500×; inset Mag: 1k×), (b) 45S5-PLGA (Mag: 770×; inset Mag: 3600×), (c) 1393-PLGA (Mag: 770×; inset: Mag: 3700×), (d) 45S5 SBF-PLGA (Mag: 200×; inset Mag: 2k×) and (e) 1393 SBF-PLGA (Mag: 2k×; inset Mag: 10k×).

carboxyl ions during the fabrication of PLGA–hydroxyapatite composite microspheres, whereas Zhou *et al.*[37] showed the existence of hydrogen bonding in the PDLLA/nano HAP composite.

However, in our opinion, the detection of ionic interaction between the filler and the matrix in composites by FTIR analysis is unreliable, and firm claims cannot be made apart from hypothetical assumptions. Recently, Ekanem *et al.*[38]

Table 3 Particle size of different microspheres

Microparticle type	d_{10} (μm)	d_{50} (μm)	d_{90} (μm)
PLGA	1.7	4.2	8.2
45S5-PLGA	4.1	20.7	62.2
45S5 SBF-PLGA	13.1	46.4	104.6
1393-PLGA	1.7	5.9	188.6
1393 SBF-PLGA	3.9	9.9	25.3

hypothesized that the polymer solution's adsorption in carbonate rocks is due to the electrostatic interaction between the calcite surface and polymer solution. The adsorption of a polymer solution also depends on mechanical entrapment on the surface of a substrate due to the presence of nano-porosity or surface roughness.

Our study proposes that the as-received bioactive glasses with low specific surface area show poor polymer wetting and entanglement during solid-in-oil-in-water emulsion. The hydrophilicity of the bioactive glasses pushes the BG particles outside of the polymer microspheres toward the continuous water based PVA phase leading to poor incorporation of bioactive glass particles into the polymer matrix during the ultrasonication-assisted emulsion process. Thus, the porous morphology of the composite microspheres is formed in the case of 45S5-PLGA and bioactive glass separated from the PLGA matrix is observed in 1393-PLGA microspheres, as shown in Fig. 4(b) and (c). When PLGA is dissolved in DCM, various surface interactions between the bioactive glass and polymeric chains could take place. It is hypothesized that due to the

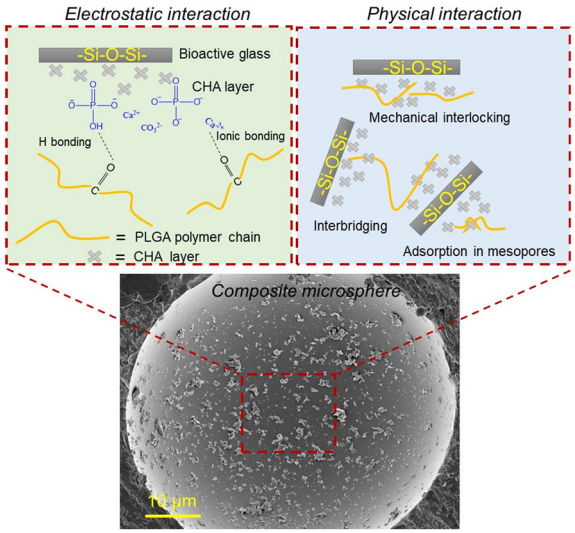

Fig. 6 Proposed electrostatic and physical interaction between the surface-treated bioactive glasses and PLGA matrix.

increase in specific surface area, which is contributed by an apparent increase in surface roughness and mesoporous type growth of CHA on the bioactive glass powders after SBF treatment, the polymer solution might have more area to diffuse and adsorb on the glass particle surface, which leads to strong physical entanglement between the polymer and surface modified filler particles as shown in Fig. 6, hence, leading to improved incorporation of the filler into the polymer matrix.

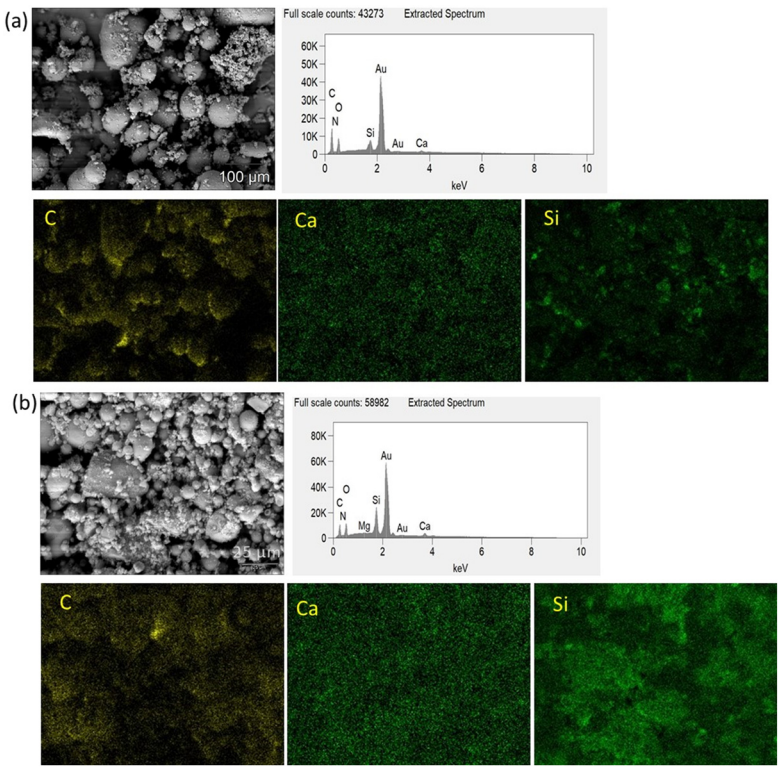

Fig. 5 EDX mapping of (a) SBF-45S5 PLGA (magnification 500×) and (b) SBF-1393 PLGA (magnification 2500×).

Our second hypothesis suggests that through SBF treatment, precipitated Ca^{2+} ions on the surface of bioactive glass might form ionic bonding with the carbonyl group present in PLGA, which also leads to strong electrostatic interaction; in addition, hydrogen bonding could also be achieved between P–OH and C═O, as shown in Fig. 6. This could contribute to better wetting of the polymeric solution with the modified glass surface. This might also be the reason for strongly agglomerated composite microspheres as shown in the inset of Fig. 4(d) and (e). This crystalline bioactive CHA layer formation on the bioactive glass could potentially improve the attachment of the bioactive glass particles onto the amorphous PLGA matrix as compared to the unmodified amorphous bioactive glass.

Conclusion and future work

In this work, we have shown the effects of SBF treatment of bioactive glasses on the surface properties of these powders. We could show that this treatment led to an increase in surface roughness and active bonding sites on nonporous melt-derived commercial bioactive glass powder particles (45S5 and 1393 in our case), which was shown to be helpful for improved incorporation of glasses in a polymer matrix during the emulsion process for composite powder fabrication. Due to the extremely low specific surface area of the melt-derived bioactive glasses, instead of using commonly exploited silane coupling agents,[39] slight nano-crystalline growth in SBF solution can activate the surface of bioactive glasses in the form of CHA precipitation to allow physicochemical interaction with the polymer matrix. In addition, SBF surface treatment acts as an environmentally friendly and easy alternative as well. In our future work, we plan to study the wetting behavior and adsorption of polyesters like PLGA and their derivatives onto different silicate-based bioactive glasses,[40] bioactive borate glasses,[41] mesoporous bioactive glasses[42] and also silica with controlled porosity like COK12.[43] The study of interaction with bio-resorbable polyesters with different chemical compositions of bioactive glasses having controlled porous structures can help improve composite fabrication for tissue engineering.

Author contributions

Nishant Jain: conceptualization, methodology, investigation, data curation, writing – original draft, writing – review & editing. Johannes Schmidt: investigation and data curation of XPS and N_2 adsorption and desorption isotherms, writing – review and editing. Oliver Görke: investigation and analysis of XRD, writing – review. David Karl: introduction writing – editing and review. Aleksander Gurlo: resources, supervision, writing – review & editing. Franziska Schmidt: conceptualization, supervision, writing – review & editing.

Conflicts of interest

There are no conflicts of interest among co-authors.

Acknowledgements

We would like to thank Laura Degenkolb from the Department of Soil Science, TU Berlin, for her support in zeta potential measurements. We would like to thank Schott AG for supplying the bioactive glass Schott Vytrixx and 1393.

References

1 W. Cao and L. L. Hench, Bioactive materials, *Ceram. Int.*, 1996, **22**, 493–507.
2 K. C. Dee, D. A. Puleo and R. Bizios, *An introduction to tissue-biomaterial interactions*, John Wiley & Sons, 2003.
3 A. Hoppe, R. Meszaros, C. Stähli, S. Romeis, J. Schmidt, W. Peukert, B. Marelli, S. N. Nazhat, L. Wondraczek, J. Lao, E. Jallot and A. R. Boccaccini, In vitro reactivity of Cu doped 45S5 Bioglass® derived scaffolds for bone tissue engineering, *J. Mater. Chem. B*, 2013, **1**, 5659–5674.
4 L. L. Hench, The story of Bioglass, *J. Mater. Sci.: Mater. Med.*, 2006, **17**, 967–978.
5 S. I. Schmitz, B. Widholz, C. Essers, M. Becker, D. U. Tulyaganov, A. Moghaddam, I. Gonzalo de Juan and F. Westhauser, Superior biocompatibility and comparable osteoinductive properties: Sodium-reduced fluoride-containing bioactive glass belonging to the CaO-MgO-SiO2 system as a promising alternative to 45S5 bioactive glass, *Bioact. Mater.*, 2020, **5**, 55–65.
6 M. Brink, The influence of alkali and alkaline earths on the working range for bioactive glasses, *J. Biomed. Mater. Res.*, 1997, **36**, 109–117.
7 I. Elgayar, A. E. Aliev, A. R. Boccaccini and R. G. Hill, Structural analysis of bioactive glasses, *J. Non-Cryst. Solids*, 2005, **351**, 173–183.
8 F. Hmood, O. Goerke and F. Schmidt, Chemical Composition Refining of Bioactive Glass for Better Processing Features, Part I, *Biomedical Glasse*, 2018, **4**(1), 82–94.
9 I. Farooq, M. Tylkowski, S. Müller, T. Janicki, D. S. Brauer and R. G. Hill, Influence of sodium content on the properties of bioactive glasses for use in air abrasion, *Biomed. Mater.*, 2013, **8**, 65008.
10 D. W. Hutmacher, Scaffolds in tissue engineering bone and cartilage, *Biomaterials*, 2000, **21**, 2529–2543.
11 K. Rezwan, Q. Z. Chen, J. J. Blaker and A. R. Boccaccini, Biodegradable and bioactive porous polymer/inorganic composite scaffolds for bone tissue engineering, *Biomaterials*, 2006, **27**, 3413–3431.
12 W. You, M. Wang and W. Lam, in *Advances in Diverse Industrial Applications of Nanocomposites*, ed. B. Reddy, InTech, 2011.
13 A. Krokos, M. Gazinska, B. Kryszak, P. Dzienny, B. Stepak, M. Olejarczyk, P. Gruber, R. Kwiatkowski, A. Bondyra and A. Antonczak, Comparison of thermal, structural and morphological properties of poly(L-lactide) and poly(L-lactide)/hydroxyapatite microspheres for laser sintering processes, *Polimery*, 2020, **65**, 605–612.

14 A. Boccaccini, Bioresorbable and bioactive polymer/Bioglass® composites with tailored pore structure for tissue engineering applications, *Compos. Sci. Technol.*, 2003, **63**, 2417–2429.
15 D. Karl, B. Jastram, P. H. Kamm, H. Schwandt, A. Gurlo and F. Schmidt, Evaluating porous polylactide-co-glycolide/bioactive glass composite microsphere powders for laser sintering of scaffolds, *Powder Technol.*, 2019, **354**, 289–300.
16 K. Zhang, Y. Wang, M. A. Hillmyer and L. F. Francis, Processing and properties of porous poly(l-lactide)/bioactive glass composites, *Biomaterials*, 2004, **25**(13), 2489–2500.
17 G. Jiang, M. E. Evans, I. A. Jones, C. D. Rudd, C. A. Scotchford and G. S. Walker, Preparation of poly(epsilon-caprolactone)/continuous bioglass fibre composite using monomer transfer moulding for bone implant, *Biomaterials*, 2005, **26**, 2281–2288.
18 Q.-Q. Qiu, P. Ducheyne and P. S. Ayyaswamy, New bioactive, degradable composite microspheres as tissue engineering substrates, *J. Biomed. Mater. Res.*, 2000, **52**, 66–76.
19 G. Conoscenti, F. Carfì Pavia, F. E. Ciraldo, L. Liverani, V. Brucato, V. La Carrubba and A. R. Boccaccini, In vitro degradation and bioactivity of composite poly-l-lactic (PLLA)/bioactive glass (BG) scaffolds: comparison of 45S5 and 1393BG compositions, *J. Mater. Sci.*, 2018, **53**, 2362–2374.
20 T. Kokubo and H. Takadama, How useful is SBF in predicting in vivo bone bioactivity?, *Biomaterials*, 2006, **27**, 2907–2915.
21 A. L. B. Maçon, T. B. Kim, E. M. Valliant, K. Goetschius, R. K. Brow, D. E. Day, A. Hoppe, A. R. Boccaccini, I. Y. Kim, C. Ohtsuki, T. Kokubo, A. Osaka, M. Vallet-Regí, D. Arcos, L. Fraile, A. J. Salinas, A. V. Teixeira, Y. Vueva, R. M. Almeida, M. Miola, C. Vitale-Brovarone, E. Verné, W. Höland and J. R. Jones, A unified in vitro evaluation for apatite-forming ability of bioactive glasses and their variants, *J. Mater. Sci.: Mater. Med.*, 2015, **26**, 115.
22 M. Plewinski, K. Schickle, M. Lindner, A. Kirsten, M. Weber and H. Fischer, The effect of crystallization of bioactive bioglass 45S5 on apatite formation and degradation, *Dent. Mater.*, 2013, **29**, 1256–1264.
23 R. Riju Chandran, S. Chitra, S. Vijayakumari, P. Bargavi and S. Balakumar, Cognizing the crystallization aspects of NaCaPO 4 concomitant 53S bioactive-structures and their imprints in in vitro bio-mineralization, *New J. Chem.*, 2021, **45**, 15350–15362.
24 H. H. Lu, S. R. Pollack and P. Ducheyne, Temporal zeta potential variations of 45S5 bioactive glass immersed in an electrolyte solution, *J. Biomed. Mater. Res.*, 2000, **51**, 80–87.
25 A. A. R. de Oliveira, D. A. de Souza, L. L. S. Dias, S. M. de Carvalho, H. S. Mansur and M. de Magalhães Pereira, Synthesis, characterization and cytocompatibility of spherical bioactive glass nanoparticles for potential hard tissue engineering applications, *Biomed. Mater.*, 2013, **8**, 25011.
26 L. M. Anovitz and D. R. Cole, Characterization and Analysis of Porosity and Pore Structures, *Rev. Mineral. Geochem.*, 2015, **80**, 61–164.
27 D. S. Brauer, Bioactive glasses—structure and properties, *Angew. Chem., Int. Ed.*, 2015, **54**, 4160–4181.
28 H. Jeffery, S. S. Davis and D. T. O'hagan, The preparation and characterisation of poly (lactide-co-glycolide) microparticles. I: Oil-in-water emulsion solvent evaporation, *Int. J. Pharm.*, 1991, **77**, 169–175.
29 M. Okada, H. Maeda, S. Fujii, Y. Nakamura and T. Furuzono, Formation of Pickering emulsions stabilized via interaction between nanoparticles dispersed in aqueous phase and polymer end groups dissolved in oil phase, *Langmuir*, 2012, **28**, 9405–9412.
30 A. Venkatakrishnan and V. K. Kuppa, Polymer adsorption on rough surfaces, *Curr. Opin. Chem. Eng.*, 2018, **19**, 170–177.
31 J. J. Blaker, V. Maquet, A. R. Boccaccini, R. Jérôme and A. Bismarck, Wetting of bioactive glass surfaces by poly(α-hydroxyacid) melts: interaction between Bioglass® and biodegradable polymers, *e-Polym.*, 2005, **5**(1), DOI: **10.1515/epoly.2005.5.1.248**.
32 R. Sergi, D. Bellucci and V. Cannillo, A review of bioactive glass/natural polymer composites: State of the art, *Materials*, 2020, **13**(23), 5560.
33 R. V. Baier, J. I. Contreras Raggio, C. M. Giovanetti, H. Palza, I. Burda, G. Terrasi, B. Weisse, G. S. de Freitas, G. Nyström, J. F. Vivanco and A. K. Aiyangar, Shape fidelity, mechanical and biological performance of 3D printed polycaprolactone-bioactive glass composite scaffolds, *Biomater. Adv.*, 2022, **134**, 112540.
34 R. E. Neuendorf, E. Saiz, A. P. Tomsia and R. O. Ritchie, Adhesion between biodegradable polymers and hydroxyapatite: Relevance to synthetic bone-like materials and tissue engineering scaffolds, *Acta Biomater.*, 2008, **4**, 1288–1296.
35 D. Yan, B. Zeng, Y. Han, H. Dai, J. Liu, Y. Sun and F. Li, Preparation and laser powder bed fusion of composite microspheres consisting of poly(lactic acid) and nano-hydroxyapatite, *Addit. Manuf.*, 2020, **34**, 101305.
36 X. Hu, H. Shen, F. Yang, X. Liang, S. Wang and D. Wu, Modified composite microspheres of hydroxyapatite and poly(lactide-co-glycolide) as an injectable scaffold, *Appl. Surf. Sci.*, 2014, **292**, 764–772.
37 S. Zhou, X. Zheng, X. Yu, J. Wang, J. Weng, X. Li, B. Feng and M. Yin, Hydrogen Bonding Interaction of Poly(dl-Lactide)/hydroxyapatite Nanocomposites, *Chem. Mater.*, 2007, **19**, 247–253.
38 E. M. Ekanem, M. Rücker, S. Yesufu-Rufai, C. Spurin, N. Ooi, A. Georgiadis, S. Berg and P. F. Luckham, Novel adsorption mechanisms identified for polymer retention in carbonate rocks, *JCIS Open*, 2021, **4**, 100026.
39 L. M. Henning, U. Simon, A. Gurlo, G. J. Smales and M. F. Bekheet, Grafting and stabilization of ordered mesoporous silica COK-12 with graphene oxide for enhanced removal of methylene blue, *RSC Adv.*, 2019, **9**, 36271–36284.
40 S. Pang, D. Wu, F. Kamutzki, J. Kurreck, A. Gurlo and D. A. Hanaor, High performing additively manufactured bone scaffolds based on copper substituted diopside, *Mater. Des.*, 2022, **215**, 110480.
41 D. Ege, K. Zheng and A. R. Boccaccini, Borate Bioactive Glasses (BBG): Bone Regeneration, Wound Healing

Applications, and Future Directions, *ACS Appl. Bio Mater.*, 2022, **5**, 3608–3622.

42 S. Kargozar, M. Montazerian, S. Hamzehlou, H.-W. Kim and F. Baino, Mesoporous bioactive glasses: Promising platforms for antibacterial strategies, *Acta Biomater.*, 2018, **81**, 1–19.

43 L. M. Henning, J. T. Müller, G. J. Smales, B. R. Pauw, J. Schmidt, M. F. Bekheet, A. Gurlo and U. Simon, Hierarchically porous and mechanically stable monoliths from ordered mesoporous silica and their water filtration potential, *Nanoscale Adv.*, 2022, **4**, 3892–3908.